

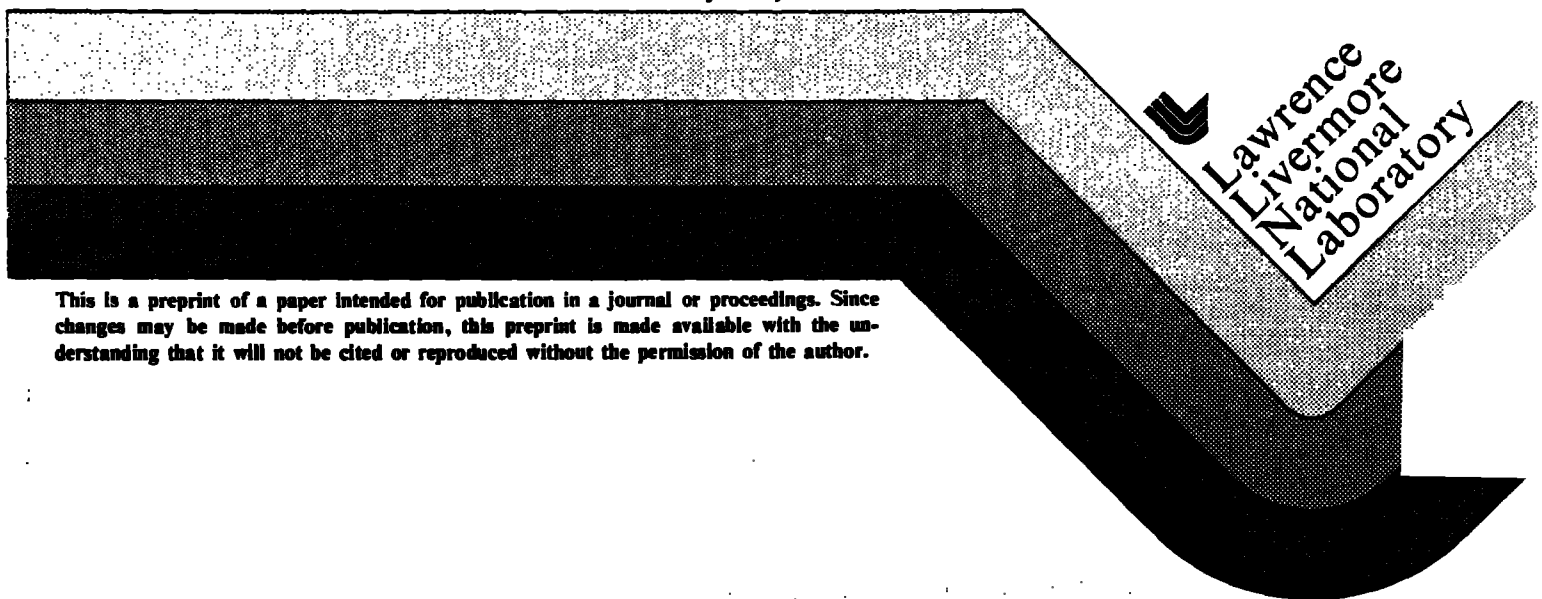
UCRL- 90835
PREPRINT

PRESSURE EFFECTS ON WALL HEAT TRANSFER DURING FLAME QUENCHING

S. R. Vosen
C. K. Westbrook

Presented at the 1984 Spring Meeting of
the Western States Section of the Combustion
Institute, University of Colorado, Boulder,
Colorado, April 2-3, 1984.

May 14, 1984



This is a preprint of a paper intended for publication in a journal or proceedings. Since changes may be made before publication, this preprint is made available with the understanding that it will not be cited or reproduced without the permission of the author.

STANDARD
AND
TECHNICAL
SERIES

DISCLAIMER

This document was prepared as an account of work sponsored by an agency of the United States Government. Neither the United States Government nor the University of California nor any of their employees, makes any warranty, express or implied, or assumes any legal liability or responsibility for the accuracy, completeness, or usefulness of any information, apparatus, product, or process disclosed, or represents that its use would not infringe privately owned rights. Reference herein to any specific commercial products, process, or service by trade name, trademark, manufacturer, or otherwise, does not necessarily constitute or imply its endorsement, recommendation, or favoring by the United States Government or the University of California. The views and opinions of authors expressed herein do not necessarily state or reflect those of the United States Government thereof, and shall not be used for advertising or product endorsement purposes.

Pressure Effects on Wall Heat Transfer During Flame Quenching

Steven R. Vosen
Sandia National Laboratories
Livermore, California 94550

Charles K. Westbrook
Lawrence Livermore National Laboratory
Livermore, California 94550

Abstract

A one-dimensional numerical model is used to predict rates of time-dependent wall heat transfer in high temperature and high pressure combustion chambers. Laminar flow near the cold wall is assumed, and global chemical kinetic mechanisms are used to describe the combustion of methane-air and propane-air mixtures. The effects of variations in fuel type, pressure, equivalence ratio, and thermal boundary layers on the wall heat flux are examined, and the calculated results are correlated in terms of characteristic time and energy units.

INTRODUCTION

The unsteady heat transfer to the walls of a combustion chamber during flame quenching is a problem of practical importance that is not well understood. Unsteady measurements have been made in a variety of devices, such as diesel engines [1,2], spark ignition engines [3,4], constant volume combustion chambers [5,6], and shock tubes [7,8]. Current combustion models, in which the unsteady one-dimensional reaction-diffusion equations are solved, are able to predict heat transfer with combustion for the lighter hydrocarbons under laminar flow conditions [5,7,8,18].

It was recently shown by Vosen [5,9] that one-dimensional unsteady calculations do very well at predicting the heat transfer as measured in a constant volume combustion chamber. For methane-air flame quenching at a cold wall, at pressures of 1 - 5 atmospheres, it was shown that detailed kinetics are not needed to predict the heat transfer, and that a global reaction scheme is sufficient. In addition, the importance of thermal boundary layers of quenching heat transfer was discussed [5].

The present study is an extension of previous work by Vosen [5] in which the present model was validated by comparison with experimental results at near-atmospheric conditions. In this paper, the same model is used to estimate heat transfer rates for flame quenching under conditions where data are much more difficult to obtain, at the high pressures and temperatures which are commonly encountered in internal combustion engines. Specifically, the heat transfer from methane-air and propane-air flames at 3.5 and 30 atmospheres pressure is predicted, and the effect of thermal boundary layers on quenching is studied.

NUMERICAL MODEL

All of the calculations were carried out using the HCT code [11]. In this program, the equations of conservation of mass, momentum, energy, and each chemical species are solved in finite difference form, for a one-dimensional planar geometry. These coupled equations are solved implicitly in time using a block tridiagonal matrix inversion technique.

In the present study the detailed chemical kinetics of the fuel oxidation are treated in a simplified manner, using one-reaction and two-reaction global reaction rates for combustion of both methane and propane in flames. This approach and the general form of the reaction rate expressions used were taken from previous work [12], in which it was shown that this model could accurately reproduce experimentally observed laminar burning velocities and flame temperatures over extended ranges of fuel-air equivalence ratio and pressure for a wide variety of hydrocarbon fuels.

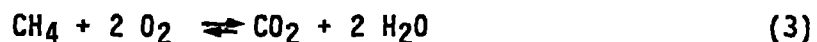
In these reaction mechanisms the rate of methane consumption is given by

$$\frac{-d[\text{CH}_4]}{dt} = k_1 [\text{CH}_4]^{0.3} [\text{O}_2]^{1.2} \quad (1)$$

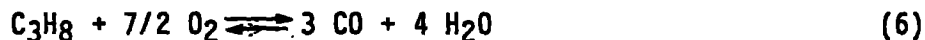
and for propane

$$\frac{-d[\text{C}_3\text{H}_8]}{dt} = k_2 [\text{C}_3\text{H}_8]^{0.1} [\text{O}_2]^{1.65} \quad (2)$$

When a single global reaction is used, the oxidation can be represented as



The use of a two-step reaction model with the HCT program provides a better estimate of the final flame temperature [12], and when such a mechanism is used, the overall reaction is broken into



followed by



In the one-reaction mechanism, $k_1 = 1.9 \times 10^{13} \exp[-48400/RT]$ and $k_2 = 4.1 \times 10^{13} \exp[-40000/RT]$, while in the two-reaction mechanism, $k_1 = 2.2 \times 10^{13} \exp[-48400/RT]$ and $k_2 = 4.8 \times 10^{13} \exp[-40000/RT]$. In addition, the rate of CO consumption in reaction 7 is adapted from Hautman et al. [13]

$$\frac{-d[\text{CO}]}{dt} = 2.66 \times 10^{14} \exp[-40000/RT] [\text{CO}]^{1.0} [\text{O}_2]^{0.25} [\text{H}_2\text{O}]^{0.5} \quad (8)$$

In order to provide an equilibrium between CO and CO₂, a reverse rate for reaction 7 is included

$$\frac{d[\text{CO}]^+}{dt} = 4.00 \times 10^8 \exp[-40000/RT] [\text{CO}_2] \quad (9)$$

Finally, to avoid numerical difficulties associated with unphysically small fuel concentrations, a reverse reaction for the fuel consumption step was included

$$\frac{d[\text{CH}_4]^+}{dt} = 1.0 \times 10^{12} \exp[-48400/RT] [\text{CO}_2]^{0.5} [\text{H}_2\text{O}] \quad (10)$$

$$\frac{d[\text{C}_3\text{H}_8]^+}{dt} = 1.0 \times 10^{16} \exp[-40000/RT] [\text{CO}] [\text{H}_2\text{O}] \quad (11)$$

The thermal diffusivity was taken from Kays and Crawford [14] and is expressed

$$\alpha = 2.0 \times 10^{-7} T^{0.669} / C_{\text{tot}} \quad (\text{cm}^2 \text{ sec}^{-1}) \quad (12)$$

where T is the local temperature and C_{tot} is the total concentration in moles-cm⁻³. In this simplified mechanism all of the chemical species are assumed to have the same molecular diffusivities, so a constant Lewis number of about 0.9 is used.

Although this type of global reaction mechanism provides reasonable flame propagation rates for freely propagating hydrocarbon flames, its adequacy in simulating the more complex problems of flame quenching and heat transfer to a cold wall were the subject of some concern. When detailed kinetic mechanisms are instead used, computed properties have been shown [10,15] to be in good agreement with available experimental results. For conditions of interest in the present work, a preliminary study was carried out to ensure that the global kinetics model agreed with the results computed from the detailed kinetic mechanism. For all of the physical parameters of concern in the present study, such as heat flux to the cold wall, overall burning rates, flame thickness, stagnation distance, and flame temperature, the global reaction approach provides good agreement with the more exact kinetics treatment, at a small fraction of the computational expense. As a result, all subsequent computations employed the global kinetics model.

Heat transfer to the combustion chamber wall is simulated by assuming first that the wall maintains a constant temperature during the quenching event. In the model, which is able to treat only gas phase phenomena, a very thin gas boundary zone is assumed to remain at the same temperature as the metal chamber wall. Heat is then removed from this boundary zone at a rate sufficient to keep it at that prescribed temperature. The computed rate of heat removal is then equal to the wall heat flux, the rate at which heat is conducted to the combustion chamber wall and subsequently removed by the appropriate cooling system. Wall heat fluxes computed in this way agree well with experimentally measured values over the 1-5 atm range studied previously [5,9].

NUMERICAL RESULTS

Flame quenching and heat transfer calculations were carried out for methane-air and propane-air mixtures at both 3.5 and 30 atmospheres pressure. The lower value was selected because it was within the range of the previous experimental study [5,9] in which only CH₄-air mixtures were used. The higher pressure was intended to be relevant to flame quenching and heat transfer in actual reciprocating engine environments. Stoichiometric, lean ($\phi = 0.8$), and rich ($\phi = 1.2$) mixtures of each fuel were included at each pressure.

The overall features of the quenching event were the same in each case. The flame approaches the wall with its direction of propagation normal to the wall. When the flame is sufficiently far (i.e. more than about 3 times the flame thickness) from the wall, the laboratory flame-speed is equal to the theoretical laminar burning velocity. During this period the computed heat flux to the wall is negligible.

As the flame begins to approach the wall, the heat flux to the wall begins to increase. The overall geometry of the flame-wall system is shown in Figure 1. The flame position can be defined in several convenient ways, two of which are indicated in Fig. 1. One of these is q_t , the location at which the gas temperature reaches a specified temperature (often 1500 K as in this figure). Another very similar definition (not shown) is the position in the flame where the temperature gradient is largest. In Fig. 1, q_r indicates the position at which the local rate of heat release from chemical reactions is largest. This definition will be used in the remainder of the present analysis, although all three definitions give nearly equivalent results.

For a short period of time as the flame approaches the wall, the model predicts that the flame actually accelerates. This acceleration is due to the difference between the rate of heat transfer to the wall and the rate at which heat is diffusing ahead of the flame. The model calculations indicate that the unburned gas between the flame and the wall is heated more rapidly than the heat can be transferred to the wall, resulting in an increased burning rate and an accelerated flame. For example, in the case of stoichiometric propane-air at 30 atm (Flame 1 in Table I), the flame has a velocity of 141 cm/sec far from the wall, accelerating to a peak value of 154 cm/sec as it approaches the wall approximately 0.01 ms before quenching.

Eventually the depletion of fuel ahead of the flame, coupled with the rapidly rising rate of heat loss to the wall, results in quenching of the flame at a distance x_0 from the wall. Computed values of this stagnation distance agree well with experimental data [10,16,17]. The detailed structure of the flame at the time of quenching, with the interactions between the radical chemistry and the perturbed temperature profile, and the kinetic mechanism responsible for flame quenching, have been discussed previously [10]. The stagnation points or quench distances, are summarized for all of the cases examined with the model in Table I.

As the flame quenches the heat flux grows rapidly. This is illustrated for Flame 1 in Fig. 2a, in which the wall heat flux q_w rises exponentially over a time period of about 2 μ sec. The flame position during this period is plotted in Fig. 2b, showing the approach of the flame to the wall, followed by a stagnation at approximately 0.0056 mm. After stagnation, the "flame" position gradually recedes from the wall. It

should be remembered that the current definition of flame position is the point at which the heat release rate has its maximum. However, the heat release rate throughout the system falls very rapidly following the time of flame quenching. In the computations, the local heat release rate due to chemical reactions was integrated in space to give a total rate of heat release due to reaction, denoted by Q_r . For a steady adiabatic flame this quantity is a constant, denoted as Q_{rad} . This quantity is plotted in Fig. 2c as a function of time relative to the time of quenching. As shown in Fig. 2c, quenching is accompanied by a substantial decrease in Q_r .

We can define a characteristic time for the heat flux variation as the interval t_q required for the heat flux to increase from 50% of its peak value to the time of its maximum value. Numerically-determined values of t_q are summarized for all of the flame models in Table 1. This time scale can be compared with a time scale related to the flame propagation given by

$$t_c = \alpha_u / S_u^2 \quad , \quad (13)$$

where α_u is the thermal diffusivity in the unburned gas. This second time scale is also shown in Table 1, where it can be seen that the characteristic time for the rise of the heat flux is between 1.5 and 2 times the flame propagation time scale. The two lower pressure flames fall in the lower end of this range while the 30-atm flames are all very similar and have a ratio of time scales close to 1.8. It is interesting to note that in this type of comparison of time scales the primary determining factor is the pressure rather than fuel type. For the 3.5 atm cases, $t_q/t_c = 1.55$, while all of the high pressure flames, regardless of fuel type or equivalence ratio, show $t_q/t_c = 1.8$.

We have already defined Q_r , the total space-integrated rate of heat release from the reactions. This quantity for a freely propagating flame will be used as the characteristic unit for normalization of the wall heat fluxes during flame quenching. For a steady, adiabatic flame,

$$\rho_u S_u \int_{T_u}^{T_b} c_p dT = \int_{-\infty}^{+\infty} (\sum_i h_i w_i) dx \quad . \quad (14)$$

Thus the quantity Q_{rad} is given by

$$Q_{rad} = \rho_u S_u \int_{T_u}^{T_b} c_p dT \equiv \rho_u S_u \bar{c}_p (T_b - T_u) \quad . \quad (15)$$

In each flame quenching event, the computed heat flux rises to a maximum value q_{wmax} at a time very shortly following the stagnation time. The computed values of q_{wmax} are summarized in Table 1 for each flame. Although the absolute values of this heat flux maximum are strongly dependent on equivalence ratio, fuel type, and pressure, when each value of q_{wmax} is normalized by its associated rate of heat release in the flame Q_{rad} , a nearly constant ratio of

$$q_{wmax} / Q_{rad} \approx 0.4 \quad (16)$$

is obtained. This ratio is given for each example in Table 1. The same ratio was obtained for lower pressure methane-air mixtures by Vosen [5,9]. Although all of the values for this wall heat flux energy ratio lie within a $\pm 5\%$ range of 0.41, closer inspection of these values suggests that the ratios for methane-air may be slightly larger than those for propane-air. This small difference, which depends on fuel type, does not appear to depend on pressure or on equivalence ratio. Recall that earlier the time scales appeared to depend on pressure but not on fuel type. In both cases, it is not possible to tell from the present modeling analysis whether these rather small differences in scaled parameters are significant or are instead produced by the simplifications in the kinetics model.

Following the time at which the wall heat flux reaches its peak value, the total rate of heat release falls rapidly (Fig. 2c) and the wall heat flux decreases roughly as the square root of the time (Fig. 2a). If the wall heat flux is normalized by Q_{rad} and the time scale is normalized by the quenching time scale t_c , all of the calculations can be reduced to a single curve. Three of these reduced variable curves are shown in Fig. 3. Independent of pressure, equivalence ratio, or fuel type, the normalized wall heat transfer rate appears to follow this curve to within $\pm 10\%$. This similarity suggests that it should be possible to use this curve, together with experimental data from freely propagating flames for other fuels at other pressures and temperatures, to predict the wall heat flux in arbitrary cases to reasonable precision.

If there is compression of the unburned gases or changes in the temperature of the wall, a thermal boundary layer will develop between the wall and the approaching flame. While these effects can be incorporated into the model, it will be shown below that the presence of a thermal boundary layer may be accounted for in a simple manner. For the one-dimensional case, consider a flame propagating in a bulk gas of temperature T_u towards an isothermal wall of temperature T_w . Even though the strength of the thermal boundary layer $(T_u - T_w)/(T_b - T_u)$ may be small, the effect of the boundary layer on the heat transfer may be considerable. A series of calculations has been carried out to illustrate this point, and to suggest possible corrections to the predicted heat transfer in the presence of thermal boundary layers. In Fig. 4 is shown the calculated heat transfer from a methane-air flame at 3.5 atm

propagating into a bulk gas of $T_u=410$ K. The dotted curve is for a wall temperature of $T_w = T_u = 410$ K. In order to simulate a thermal boundary layer the calculation was repeated, but the wall temperature was lowered from $T_w = 410$ K to $T_w = 300$ K at a time 2 ms before the maximum heat flux occurred in the first calculation (that is, $t_{qmax}-t = 2$ ms). The result is a developing thermal boundary layer which is several times the flame thickness when quenching occurs. The results from this calculation are shown as the solid curve in Fig. 4. By lowering the wall temperature by 6 % of the total temperature difference across the flame, q_{wmax} has decreased by 20 % and the time for quenching to occur has increased by 64 %. An examination of the results of the calculation suggests the following explanation. The small change in the temperature has little effect on the temperature profile in the gas, but it has a large effect on the thermal properties of the gas near the wall. For example, the maximum heat flux as a function of the wall temperature $q_w(T_w)$ without a thermal boundary layer (i.e. at $T_w=T_u$) is given by:

$$q_{w \max}(T_u) = -k_w \frac{\partial T}{\partial x} \Big|_w = -k_u \frac{\partial T}{\partial x} \Big|_w \quad (17)$$

The thermal boundary layer has little effect on the temperature gradient at the wall $\frac{\partial T}{\partial x} \Big|_w$, but it changes k_w , the thermal conductivity at the wall, by an appreciable amount. Thus the maximum wall heat flux for a wall temperature T_w is given by

$$\begin{aligned} q_{w \max}(T_w) &= -k_w \frac{\partial T}{\partial x} \Big|_w \\ &= \frac{k_w}{k_u} q_{w \max}(T_u) \end{aligned} \quad (18)$$

It was shown above that $q_{w\max}(T_u)$, that is in the absence of a thermal boundary layer, is proportional to Q_{rad} . Thus

$$\frac{q_{w\max}(T_w)}{Q_{\text{rad}}} = \frac{k_w}{k_u} \frac{q_{w\max}(T_u)}{Q_{\text{rad}}} \equiv c_1 \frac{k_w}{k_u} \quad . \quad (19)$$

Likewise, we assume that T_w has little effect on the temperature profile near the wall at the quench distance

$$t_q(T_w) \sim \frac{\delta^2(T_w)}{\alpha_w} \sim \frac{\delta^2}{\alpha_w} \quad , \quad (20)$$

and

$$t_q(T_w) = \frac{\alpha_u}{\alpha_w} t_q(T_u) \quad . \quad (21)$$

The value of $t_q(T_u)$ in the absence of a thermal boundary layer was shown above to be proportional to t_c , so that

$$\frac{t_q(T_w)}{t_c} = \frac{\alpha_u}{\alpha_w} \frac{t_q(T_u)}{t_c} \equiv c_2 \frac{\alpha_u}{\alpha_w} \quad . \quad (22)$$

Correcting for the thermal boundary layer by plotting $q_w k_w / k_u$ against $t \alpha_u / \alpha_w$, as suggested by Equations 19 and 22, results in the curve shown in Fig. 5. Again, the dotted curve is for the case where $T_w = T_u$ (and thus the curve is just q_w vs. t). The solid curve is for the case where $T_w = T_u$.

These corrections were also applied to experimental data [5] obtained in a constant volume combustion chamber. The thermal boundary layer in that chamber was due to the adiabatic compression of the unburned gases and resulted in a boundary layer several times the flame thickness. It was concluded that when equations 19 and 22 were applied to the data, the predictions of the model in the absence of the thermal boundary agreed with the experimental data.

In the work of Isshiki and Nishiwaki [6], the maximum heat flux and the time for quenching were measured for H₂-O₂ flames in a constant volume combustion chamber (and thus thermal boundary layers were present). The data could be correlated by a relation which may be written as [5]

$$\frac{q_{w \max}(T_w)}{Q_{\text{rad}}} \sqrt{\frac{t_q(T_w)}{t_c}} = \text{const} \quad (23)$$

Combining the results of this work in the absence of thermal boundary layers and the correction due to the boundary layer gives

$$\begin{aligned} \frac{q_{w \max}(T_w)}{Q_{\text{rad}}} \sqrt{\frac{t_q(T_w)}{t_c}} &= \frac{q_{w \max}(T_u)}{Q_{\text{rad}}} \frac{k_w}{k_u} \sqrt{\frac{t_q(T_u)}{t_c}} \frac{\alpha_u}{\alpha_w} \\ &= \left[\frac{q_{w \max}(T_u)}{Q_{\text{rad}}} \right] \sqrt{\frac{t_q(T_u)}{t_c}} \left(\sqrt{\frac{(k\rho c_p)_w}{(k\rho c_p)_u}} \right) \\ &= c_1 \sqrt{c_2} \left(\sqrt{\frac{(k\rho c_p)_w}{(k\rho c_p)_u}} \right) \quad (24) \end{aligned}$$

The quantity in parentheses is a slowly varying function of temperature, and the contribution from this term is negligible compared to the experimental error. Thus the results of this work compare well with the correlation of Isshiki and Nishiwaki.

Thus it appears that most of the effects of the thermal boundary layer on the wall heat transfer are a result of variations in the thermal properties at the wall. The changes in the maximum heat flux and time for quenching are given by Equations 19 and 22, and may be combined to give Equation 23. In addition, using the scaling of the time and heat flux as suggested by Equations 19 and 22, the variation of the heat flux with time in the presence of a thermal boundary layer may be realistically interpreted as shown in Figures 4 and 5.

DISCUSSION

The computational analysis in the present paper has been verified experimentally only at the very lowest end of the pressure range considered, below 5 atm [5,9]. Several important tests of its applicability and accuracy should be carried out. One of these involves the use of fuels besides methane, such as propane and ethylene. Since the laminar burning velocity of ethylene-air is significantly greater than that of methane-air and the flame thickness is correspondingly smaller, the use of ethylene would provide an interesting test of the validity of the current results, at least for the low pressure range between 1 and 5 atmospheres. Extension of the pressure range beyond 5 atm is more difficult but would provide an even more valuable test of the current approach.

The practical application of these results to real combustion systems is dependent on the importance of the errors which result from the simplifications introduced into the model. Probably the most significant of these is the treatment of the wall boundary layer. The results presented here indicate that the differences between wall heat fluxes predicted without considering the boundary layer can be significant. This clearly identifies the boundary layer as an important factor in the process of wall heat transfer. As we have shown, some of the influence of the thermal boundary layer can be included in the present model, but further analysis is needed.

All of these calculations assume laminar flow normal to the wall boundary. The influences of turbulence and shear flows near the boundary are therefore not included and may be of considerable importance in

determining the wall heat transfer in practical combustors such as internal combustion engines. The success of the laminar flow assumption in predicting flame quenching distances [10], which agreed well with experimental results in real engine environments [16], suggests that the present numerical estimates may not be grossly in error. Experimental heat transfer data from internal combustion engines [1-4] show for q_w which are smaller than the peak values predicted here by about an order of magnitude. However, the time scales over which the present computations estimate these high heat transfer rates are very short. For example, for Flame 1 in Table 1, the wall heat flux rises by two orders of magnitude in less than $10 \mu s$, about 0.01 crankangle degrees at 2000 rpm. Considering the fact that cycle-to-cycle variations in flame arrival time are an important factor in engine measurements, together with the fact that temporal resolution of less than 0.01 crankangle degrees would be needed to resolve the wall heat flux, it is not surprising that the available experimental data do not exhibit the same peak wall heat flux values that are predicted by the model. On the other hand, the time scale over which the model predicts this high wall heat flux is also very short, so its effect on the time integrated wall heat transfer is quite small.

ACKNOWLEDGMENTS

We are grateful to Professor Ralph Greif of the University of California at Berkeley for many contributions to this work. This work was carried out under the auspices of the U. S. Department of Energy at Sandia National Laboratories under contract No. DE-AC03-76SF00098 and at Lawrence Livermore National Laboratory under contract No. W-7405-ENG-48.

REFERENCES

1. Woschni, G., "A Universally Applicable Equation for the Instantaneous Heat Transfer Coefficient in the Internal Combustion Engine", SAE Transactions 76, 3065 (1967).
2. Annand, W.J.D., "Heat Transfer in the Cylinders of Reciprocating Internal Combustion Engines", Proc. Inst. Mech. Eng. 177, 973 (1963).
3. Alkidas, A.C., "Heat Transfer Characteristics of a Spark-Ignition Engine", J. Heat Transfer 102, 189 (1980).
4. Overbye, V.D., Bennethum, J.E., Uyehara, O.A., and Myers, P.S., "Unsteady Heat Transfer in Engines", SAE Transactions 69, 461 (1961).
5. Vosen, S.R., "Unsteady Heat Transfer During the Interaction of a Laminar Flame with a Cold Wall", Ph. D. thesis, University of California at Berkeley, 1983.
6. Isshiki, N., and Nishiwaki, N., "Basic Study on Inside Convective Heat Transfer of Internal Combustion Engines", Proc. Fifth Int. Heat Transfer Conf. II, 344 (1974).
7. Keipur, R., and Spurk, J.H., "Methane Oxidation Near a Cold Wall", J. Fluid Mech. 113, 333 (1981).
8. Heperkan, H.A., "An Experimental and Theoretical Study of Heat Transfer with Combustion", Ph. D. thesis, University of California at Berkeley, 1980.
9. Vosen, S.R., Greif, R., and Westbrook, C.K., "Unsteady Heat Transfer During Laminar Flame Quenching", to be presented at the Twentieth International Symposium on Combustion, Ann Arbor, Michigan, August 1984.
10. Westbrook, C.K., Adamczyk, A.A., and Lavoie, G.A., "A Numerical Study of Laminar Flame Wall Quenching", Combust. Flame 40, 81 (1981).
11. Lund, C.M., "HCT-A General Computer Program for Calculating Time-Dependent Phenomena Involving One-Dimensional Hydrodynamics, Transport, and Detailed Chemical Kinetics", Lawrence Livermore National Laboratory report UCRL-52504, 1978.
12. Westbrook, C.K., and Dryer, F.L., "Simplified Reaction Mechanisms for the Oxidation of Hydrocarbon Fuels in Flames", Combust. Sci. Tech. 27, 31 (1981).
13. Hautman, D.L., Dryer, F.L., Schug, K.P., and Glassman, I., "A Multiple-Step Overall Kinetic Mechanism for the Oxidation of Hydrocarbons", Combust. Sci. Tech. 25, 219 (1981).

14. Kays, W.M., and Crawford, M.E., Convective Heat and Mass Transfer, second edition, McGraw-Hill, New York (1980).
15. Sloane, T.M., and Schoene, A.Y., "Computational Studies of End-Wall Flame Quenching at Low Pressure: The Effects of Heterogeneous Radical Recombination and Crevices", Combust. Flame **49**, 109 (1983).
16. Daniel, W.A., "Flame Quenching at the Walls of an Internal Combustion Engine", Sixth Symposium (International) on Combustion, Reinhold, New York, 1957.
17. Blint, R.J., and Bechtel, J.H., "Flame/Wall Interface: Theory and Experiment", Combust. Sci. Tech. **27**, 87 (1982).
18. Kurkov, A.P., "A Theoretical Study of Flame Extinction by a Cold Wall and Flame Ignition by a Hot Surface", Ph. D. thesis, University of Michigan (1967).

Table I

Flame	Fuel	ϕ	P atm	T _u K	T _b K	S _u cm/s	t _c μ s	t _q μ s	t _q /t _c	Q _{rad} MW/m ²	q _{w max} MW/m ²	$\frac{q_{w \max}}{Q_{\text{rad}}}$	x _o mm
1	C ₃ H ₈	1.0	30	793	2733	189	1.06	1.89	1.78	71.7	28.3	.395	0.0056
2	C ₃ H ₈	1.0	3.5	429	2417	65	27.50	42.90	1.56	5.24	2.07	.395	0.066
3	CH ₄	1.0	30	793	2691	121	2.58	4.63	1.79	42.1	17.4	.413	0.0091
4	CH ₄	1.0	3.5	429	2409	50	46.40	71.90	1.55	3.76	1.53	.407	0.092
5	C ₃ H ₈	1.2	30	793	2663	180	1.17	2.15	1.84	65.7	25.8	.393	0.0059
6	C ₃ H ₈	0.8	30	793	2446	74	6.84	1.26	1.83	22.9	8.88	.388	0.0154
7	CH ₄	1.2	30	793	2625	116	2.81	4.72	1.68	40.0	17.0	.424	0.0094
8	CH ₄	0.8	30	793	2388	93	4.36	7.41	1.70	26.3	11.6	.441	0.0115

FIGURE CAPTIONS

1. Schematic view of the flame-wall interaction, showing the temperature profile (solid curve), the rate of heat release due to chemical reactions (dashed curve), a graphical definition of the flame thickness L_t in terms of the temperature gradient, and the two definitions of the flame position described in the text.
2. Results of the calculations described in the text for the quenching of a propane-air flame ($\phi = 1.0$, $P = 30$ atm, $T_u = 793$ K). The three parts of the figure show the variation with time of the flame position (Fig. 2a), the wall heat flux (Fig. 2b), and the total amount of chemical heat release in the flame.
3. The wall heat flux during quenching for three flames: propane-air, $\phi = 1.0$, $P = 30$ atm, $T_u = 793$ K (solid line); propane-air, $\phi = 1.0$, $P = 3.5$ atm, $T_u = 429$ K (dashed line); methane-air, $\phi = 1.0$, $P = 30$ atm, $T_u = 793$ K (dotted line). The results have been rendered nondimensional by the characteristic time and heat flux for steady flame propagation.
4. Wall heat flux as a function of time for quenching for the same flame without a pre-existing thermal boundary layer (dotted line), and with a thermal boundary layer (solid line).
5. Wall heat flux as a function of time showing the effect of thermal boundary layers on quenching. When the heat flux in the presence of a thermal boundary layer is modified by the ratio of the thermal properties across the flame (solid line) the results are very similar to the results for quenching without a thermal boundary layer (dotted line).

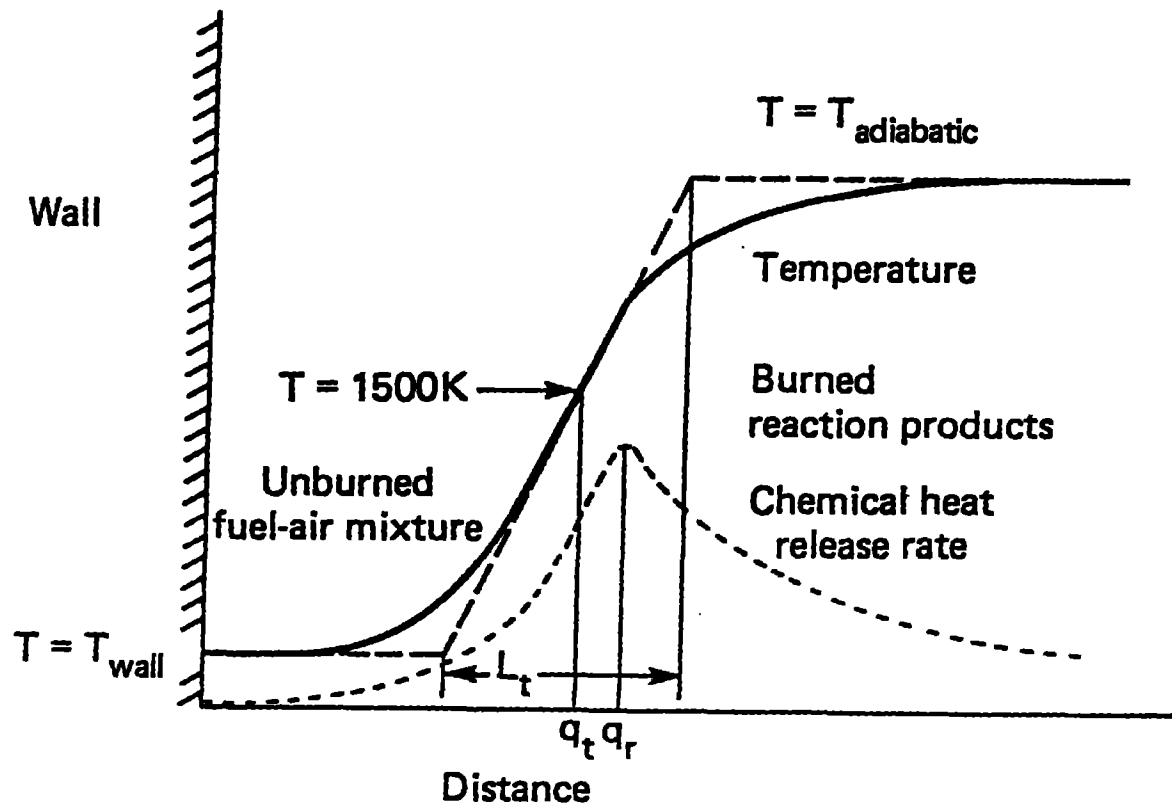


Figure 1

Figure 2a

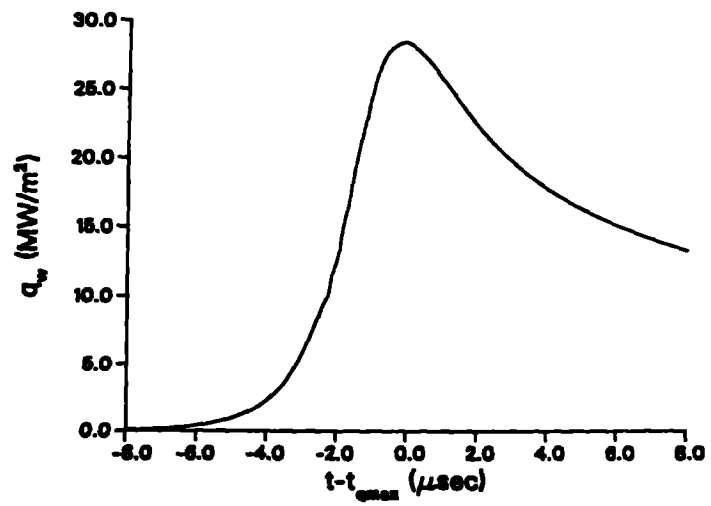


Figure 2b

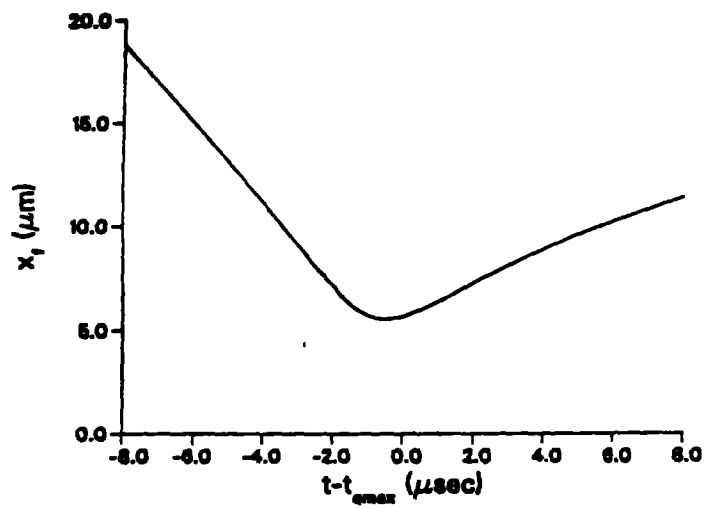


Figure 2c

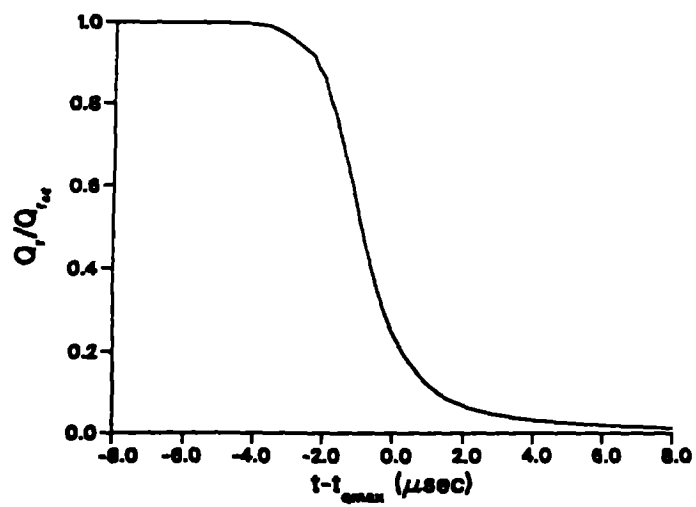


Figure 3

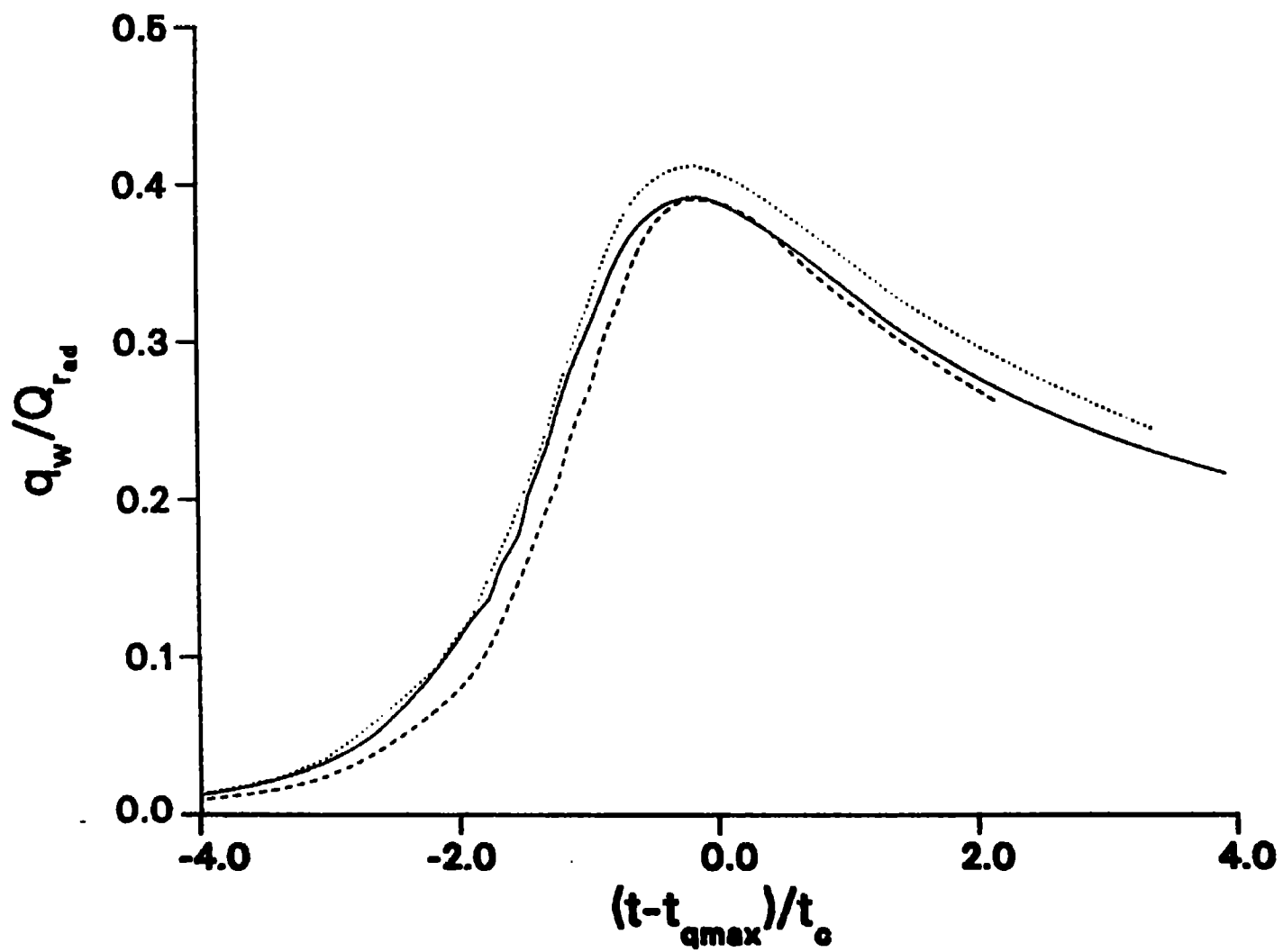


Figure 4

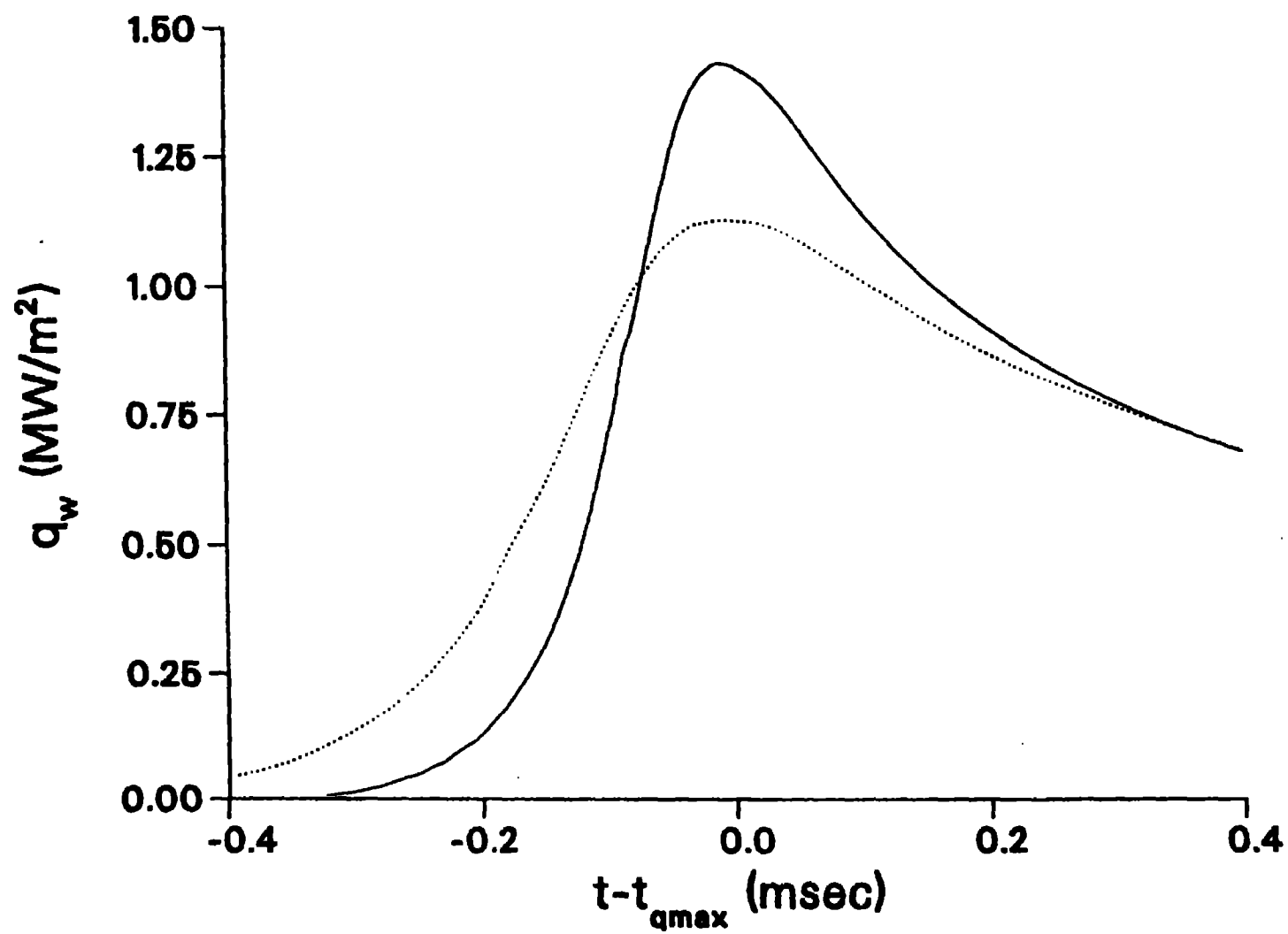


Figure 5

